Methods

Mouse studies

Adult female mice were subjected to timed pregnancies and were scored by the presence of vaginal plugs, with 9:00am on the day of plug detection designated as 0.5 days post coitum. For excision of floxed alleles using the *Prox1-Cre*^{ERT2} line, tamoxifen (20 mg/mL; Sigma) was dissolved in peanut oil containing 10% ethanol. Pregnant mice were injected intraperitoneally with 2.5 mg per 25g of body weight at the indicated time points.

Cell culture experiments

Adult human dermal lymphatic microvascular endothelial cells HMVEC-dLyAd (hLEC) and adult human dermal blood microvascular endothelial cells HMVEC-dBlAd (hBEC) were purchased from Lonza and cultured in EGM-2MV medium (Lonza). HEK293 cells (a gift from Stuart Pitson, SA Pathology, Adelaide) were maintained in DMEM medium with high glucose containing 10% FBS. K562 cells (a gift from Junia Melo, SA Pathology, Adelaide) were maintained in RPMI containing 10% FBS. Flow experiments with hLEC were performed as described previously (1). Briefly, hLEC were transfected with 66nM of siRNA using Lipofectamine RNAimax (Invitrogen). siRNA used were Qiagen AllStars Negative Control siRNA (Qiagen 1027281) and SMARTpool: ON-TARGETplus *GATA2* siRNA (Dharmacon L-009024-02). Following transfection, hLEC were seeded at confluence on fibronectin-coated slides (μ-Slide I 0.8 Luer; ibidi), cultured for 24 hours and subjected to oscillatory or laminar flow (4 dynes/cm^2, 1/4 Hz) in a parallel plate flow chamber system (ibidi Pump System; ibidi), or kept under static conditions for 48 hours. At the end of the experiment, cells were fixed and processed for immunofluorescent immunostaining. For quantification of nuclear immunostaining intensity, 25-100 nuclei from each of four independent experiments were outlined, based on DAPI staining, and nuclear area and staining intensity were measured in

ImageJ (2) using the “analyze particles” function. In total, 250 cells were analysed per condition. To allow comparison across independent experiments, nuclear intensity in shear stress condition was normalized to the expression level under static conditions in the same experiment, which was set to 1.

Antibodies

For immunofluorescent immunostaining, the primary antibodies used were rabbit anti-Gata2 (Santa Cruz, sc-9008), rabbit anti-Gata2 (Novus, NBP1-82581), rabbit anti-Prox1 (AngioBio, 11-002), rabbit anti-LYVE-1 (AngioBio, 11-034), goat anti-Prox1 (R&D Systems, AF2727), rat anti-CD31 (BD Pharmingen, 553370), hamster anti-podoplanin (Developmental Studies Hybridoma Bank, 8.1.1), rat anti-Endomucin (Santa Cruz, sc-65495), goat anti-Nrp2 (R& D Systems, AF2215), rabbit anti-Nrp2 (Cell Signaling, D39A5), goat anti-VE-cadherin (R&D Systems, AF1002), mouse anti-β-catenin (BD Transduction Laboratories, #610154), APC Mouse Lineage Antibody Cocktail (BD Biosciences, 558074), Cy3-conjugated mouse monoclonal anti-α smooth muscle actin (Sigma, C6198), rat anti-Foxc2 (3), rabbit anti-Ki67 (Abcam, ab15580) and rabbit anti-β-galactosidase (MP Biomedicals, #55976). Alexa Fluor fluorochrome-conjugated antibodies were used for detection (Molecular Probes, Life Technologies). For ChIP and WEMSA, antibodies used were rabbit anti-Gata2 (Santa Cruz, sc9008X), goat anti-Foxc2 (Abcam, ab5060), rabbit anti-Nfatc1 (Santa Cruz, sc13033X), rabbit anti-H3K4Me1 (Cell Signaling, #5326), rabbit anti-H3K27Me3 (Cell Signaling, #9733) and rabbit IgG (Cell Signaling #2729). For immunoprecipitation and immunoblotting, mouse monoclonal anti-GATA2 (Santa Cruz, sc-267), mouse anti-Myc (Cell Signaling, #2276), rabbit anti-Nfatc1 (Santa Cruz, sc13033), goat anti-Prox1 (R&D Systems, AF2727), mouse anti-β-actin (Sigma, A5441) and rabbit IgG (Santa Cruz, sc-2027) antibodies were used.

Evans Blue injections

25 μl of Evans Blue (1% w/v in phosphate buffered saline) was injected into the footpads of anaesthetised, littermate-matched mice between 3 and 6 months of age. Animals were humanely killed after 60 minutes and dissected to examine Evans Blue transport via collecting vessels to the thoracic duct. Thoracic duct area was measured by analysing images at identical magnification and selecting equal lengths of thoracic duct spanning approximately six ribs. ImageJ (2) was used to quantify the number of pixels bounded by the area of the thoracic duct.

Immunostaining

For frozen sections and whole mount staining of skin, embryos were fixed in 4% paraformaldehyde overnight at 4°C. For whole mount staining of mesentery, embryos were dissected, mesenteries removed and fixed in 4% paraformaldehyde for 10 minutes at room temperature. Sections and tissues were immunostained and imaged using confocal microscopy as previously described (4). Images were captured at room temperature using a Zeiss LSM 700 confocal microscope (Zeiss Laboratories) equipped with four solid lasers (near UV 405, Green 488nm, Red 555nm and Far Red Diode 637nm) and a Zeiss inverted Axio Observer Z1 fluorescence microscope. Images were compiled using ZEN lite 2011 (blue edition) version 1.0 (Carl Zeiss) and Adobe Photoshop CS5 version 12.0 (Adobe) software.

Plasmids and Mutagenesis

Gata2 WT and mutant allelic series expression vector constructs were made by cloning open reading frames into pCMV-Entry (Origene) (5). For luciferase reporter constructs, genomic DNA regions of interest were generated using PCR, cloned into pGL4.12 (Promega, GenBank Accession no. AY738224) and sequences verified. Chromosomal coordinates of the genomic regions and primers used for amplification were as follows:

Prox1 -11 kb enhancer: GRCm38/mm10 Chr1:190181703-190182534 (832bp).

Forward 5'- GGCAAGCATGGGCATGGTGGAT-3', Reverse 5'- AGCATGGCCTTGAGGCTCGGT-3'.

Foxc2 (Gata2-ChIP) peak: GRCh37/hg19 Chr16:86617698-86618543 (8

Forward 5'- CAGAGCTGGAGTGGAAAGGA- 3', Reverse 5'- GGTGGGAGAGTCACTTGAGG-3'.

Prox1 +4.5 kb: GRCm38/mm10 Chr1:190162262-190166213 (3925 bp, a gift from Mat Francois, Institute for Molecular Bioscience, The University of Queensland, Brisbane).

Prox1 +4.5 kb (subclone): GRCm38/mm10 Chr1:190162266-190163808 (1543bp) Forward 5'- TGCAGGTTATTTCATGCTGAA- 3', Reverse 5'- CATCTTCAAAAGCTCGTCAGC-3'.

Mutations in luciferase reporter constructs were introduced using the QuikChange Site-Directed Mutagenesis Kit, as per manufacturer's instructions (Stratagene).

Luciferase Assays

HEK293 cells were transfected in triplicate using Lipofectamine 2000 (Life Technologies) according to manufacturer's instructions and harvested 24 hours post-transfection. Luciferase levels in cell lysates were measured using the Luciferase Assay System and GloMax-Multi+ Detection System (Promega), as per manufacturer's directions.

Western Blot-Electrophoretic Mobility Shift Assay

WEMSAs were performed as previously described (5). Briefly, HEK293 cells were transfected with wild-type or mutant GATA2 constructs using Lipofectamine 2000 (Life Technologies) according to manufacturer's instructions and harvested 24 hours post-transfection. Nuclear extracts were then prepared using a NE-PER® Nuclear and Cytoplasmic Extraction kit (Pierce)

according to manufacturer's instructions. Double stranded DNA oligonucleotides containing GATA binding sites present in the *Prox1* +4.5 kb and -11 kb elements were synthesised and labelled using a Biotin 3' End DNA Labeling kit (Pierce) and annealed according to the manufacturer's protocol. Double stranded labelled probes (100 fmol) were incubated with 3 μg of nuclear extract for 20 min in binding buffer (20 mM HEPES-KOH, pH 7.9, 100 mM KCl, 2 mM MgCl2, 10 μM ZnSO4, 10 mM 2 mercaptoethanol, 0.1% NP-40, 10% glycerol, 0.2 mM EDTA and 5 μg/ml sheared salmon sperm DNA). Polyclonal rabbit anti-GATA2 (H-116) antibody (Santa Cruz, sc-9008) (1:100) was added to nuclear lysates for 20 min prior to addition of probe to demonstrate GATA2 as the binding protein. To assess the specificity of the binding, 200-fold excess of each unlabeled probe was used as competitor. Complexes were resolved in 6% non-denaturing polyacrylamide gels made in 0.5x TGE buffer (12.5 mM Tris-HCl, pH 8.5, 85 mM glycine and 0.5 mM EDTA) at 4°C. Shifted DNA oligonucleotide/protein complexes were transferred onto nitrocellulose membrane, and the membrane was probed with mouse monoclonal anti-GATA2 (CG2-96) antibody (Santa Cruz, sc-267). Detection was performed using a Chemiluminescent Nucleic Acid Detection Module (Pierce) according to the manufacturer's protocol.

Chromatin Immunoprecipitiation

hLEC, hBEC and K562 cells were harvested and processed for ChIP using a truChIP™ Low Cell Chromatin Shearing Kit with SDS Shearing Buffer (Covaris). Briefly, 10 million cells/ml were cross-linked using 1% formaldehyde for 5 minutes, neutralised with glycine, lysed and nuclei washed. For transcription factor ChIP, chromatin from 3 million cells was sheared using a 130μl microtube in a Covaris sonicator at the recommended settings for 8 minutes. 5μg antibody or IgG control was used to immunoprecipitate sheared DNA. For histone mark ChIP, chromatin from 1 million cells was sheared and 1μg antibody/IgG control was used. Following

washing and reversal of crosslinks, DNA was purified using a Qiagen MinElute PCR Purification Kit and recovery of *PROX1* -11kb enhancer sequences analysed by qPCR using a Roche LightCycler 480 and Universal Probe Library (human) probe #43 with specific primers as follows: Forward 5'-AGCCAGGGAATGAGTACAGG-3' Reverse 5'-AGGAAGCCTGTGCATTAACAC-3'.

ChIP-Seq Analysis

ChIP-Seq library preparation and sequencing was carried out at the ACRF Cancer Genomics Facility, Centre for Cancer Biology, Adelaide. ChIP-Seq libraries were prepared according to Illumina's TruSeq Sample Prep Guide Revision A with some minor modifications. Briefly, DNA was end-repaired, followed by adenylation of the 3' ends. Next, Illumina indexing adapters were ligated to the DNA. 18 cycles of PCR was performed to enrich for successfully adapter ligated molecules. Ligation products were purified with a 2% Pippin Prep gel (Sage Science), selecting a size range of 250 – 300 base pairs. The size distribution and yield of the purified libraries were determined using an Agilent Bioanalyzer High Sensitivity chip and Qubit dsDNA HS assay (Invitrogen), respectively. Libraries were pooled in equimolar ratios and sequenced in one lane of a HiSeq 2500 short read flowcell (1 x 50bp). Reads were mapped to the UCSC hg19 genome with BWA (6) version 0.7.9a-r786, allowing at most 3 alignments. Read depth was calculated via genomeCoverageBed from BEDTools (7), using the scale parameter to normalise to reads-per-million. Read depth was plotted relative to annotated transcription start sites via custom Python scripts utilising Matplotlib (8).

Immunoprecipitation and Immunoblotting.

To analyse protein interactions, HEK293 cells were co-transfected with Gata2, Nfatc1-Myc and Foxc2-Myc expression vectors (all in pCMV6-ENTRY, OriGene) using Lipofectamine

2000 (Invitrogen). 24 hours post transfection, cells were lysed with buffer containing 20 mM Tris pH 7.5, 500 mM NaCl, 1% IGEPAL® CA-630 supplemented with Halt™ Protease and Phosphatase Inhibitor Cocktail (Thermo Scientific). Lysates were sonicated, centrifuged, and then incubated overnight with respective primary antibodies (anti-GATA2, Santa Cruz, anti-NFATC1, Santa Cruz) or control IgG (Santa Cruz). Antibody-antigen complexes were incubated with Dynabeads® Protein A (Life Technologies) and the immunoprecipitates washed with lysis buffer, resuspended in Laemmli sample buffer, and heated at 95 ºC for 5 min. For immunoblotting, samples were resolved by SDS-PAGE, transferred to PVDF (PerkinElmer) and blotted with respective antibodies. Immunoblots were visualized using ECF reagent (GE Healthcare) and a Typhoon FLA 9000 (GE Healthcare).

GATA2 C-terminal zinc finger protein production, purification and characterization.

Wild-type and mutant human GATA2 C-terminal zinc finger (CF; residues 328–409) were expressed and purified as described for the GATA1 N-terminal zinc finger construct (9), with the exception that 20 mM Tris (pH 8.5) was maintained throughout the buffers, and a single cation exchange step, using a 50–600 mM NaCl step gradient was used. Proteins were >90% pure as judged by SDS-PAGE (Supplemental Figure 4) and protein concentrations were determined by $A_{280\ nm}$ based on extinction coefficients of 14.0 $cm^{-1}.mM^{-1}$ for the R398W mutant, and 8.48 $cm^{-1}.mM^{-1}$ for WT and all other mutants. GATA2-CF proteins were dialysed into 20 mM sodium phosphate (pH 7.4), 50 mM NaCl, 1 mM DTT. Far-UV circular dichroism spectra (CD; 195–260 nm) were collected on 5 μM protein using a JASCO J-815 CD spectropolarimeter at 25 °C. The resulting spectra were smoothed in Origin (Microcal) five-point fast Fourier transform filtering. One-dimensional proton (1D-H^1) NMR spectra were collected (using the same buffer and temperature) on a Bruker AvanceIII 800 MHz

spectrometer on samples (150–300 μM CF protein) supplemented with 10 % (v/v) D_2O, and 17 μM 4,4-dimethyl-4-silapentane-1-sulfonic acid (DSS) as an internal reference.

Electrophoretic Mobility Shift Assays (EMSA)

GATA2 C-terminal zinc finger proteins were tested for their DNA-binding capacity by EMSA with a GATA site-containing fluorescein (FAM) labelled oligo derived from the -11 kb regulatory region of the murine *Prox1* gene (5'-CCCAGCCGCTCCA**GATA**AGAGGTGGCCGTG -3'; FAM-Prox1). Proteins were dialysed into 20 mM Tris (pH 7.9), 50 mM NaCl, 1 mM DTT, and combined at concentrations between 50 nM–6.4 μM with FAM-Prox1 (5 nM) in the above buffer supplemented with 0.2 mg/ml BSA and 5 mM $MgCl_2$. Samples were incubated on ice for 30 min, separated on 8% non-denaturing polyacrylamide gels made in 0.5x TBE (45 mM Tris, 45 mM Boric acid, 2.5 mM EDTA) and visualised using a Typhoon FLA 9000 laser scanner equipped with a 473 nm laser and a LPB filter set.

Supplemental References

1. Sabine A, Agalarov Y, Maby-El Hajjami H, Jaquet M, Hagerling R, Pollmann C, Bebber D, Pfenniger A, Miura N, Dormond O, et al. Mechanotransduction, PROX1, and FOXC2 cooperate to control connexin37 and calcineurin during lymphatic-valve formation. *Dev Cell.* 2012;22(2):430-45.
2. Abramoff M, Magalhaes, PJ, Ram, SJ. Image processing with ImageJ. *Biophotonics International.* 2004;11(7):36-42.
3. Furumoto TA, Miura N, Akasaka T, Mizutani-Koseki Y, Sudo H, Fukuda K, Maekawa M, Yuasa S, Fu Y, Moriya H, et al. Notochord-dependent expression of MFH1 and PAX1 cooperates to maintain the proliferation of sclerotome cells during the vertebral column development. *Dev Biol.* 1999;210(1):15-29.
4. Kazenwadel J, Secker GA, Liu YJ, Rosenfeld JA, Wildin RS, Cuellar-Rodriguez J, Hsu AP, Dyack S, Fernandez CV, Chong CE, et al. Loss-of-function germline GATA2 mutations in patients with MDS/AML or MonoMAC syndrome and primary lymphedema reveal a key role for GATA2 in the lymphatic vasculature. *Blood.* 2012; 119(5):1283-91.
5. Hahn CN, Chong CE, Carmichael CL, Wilkins EJ, Brautigan PJ, Li XC, Babic M, Lin M, Carmagnac A, Lee YK, et al. Heritable GATA2 mutations associated with familial myelodysplastic syndrome and acute myeloid leukemia. *Nat Genet.* 2011;43(10):1012-7.
6. Li H, and Durbin R. Fast and accurate short read alignment with Burrows-Wheeler transform. *Bioinformatics.* 2009;25(14):1754-60.
7. Quinlan AR, and Hall IM. BEDTools: a flexible suite of utilities for comparing genomic features. *Bioinformatics.* 2010;26(6):841-2.

8. Hunter JD. Matplotlib: A 2D graphics enivornment. *Computing In Science & Engineering.* 2007;9(3):90-5.

9. Wilkinson-White L, Gamsjaeger R, Dastmalchi S, Wienert B, Stokes PH, Crossley M, Mackay JP, and Matthews JM. Structural basis of simultaneous recruitment of the transcriptional regulators LMO2 and FOG1/ZFPM1 by the transcription factor GATA1. *Proc Natl Acad Sci U S A.* 2011;108(35):14443-8.

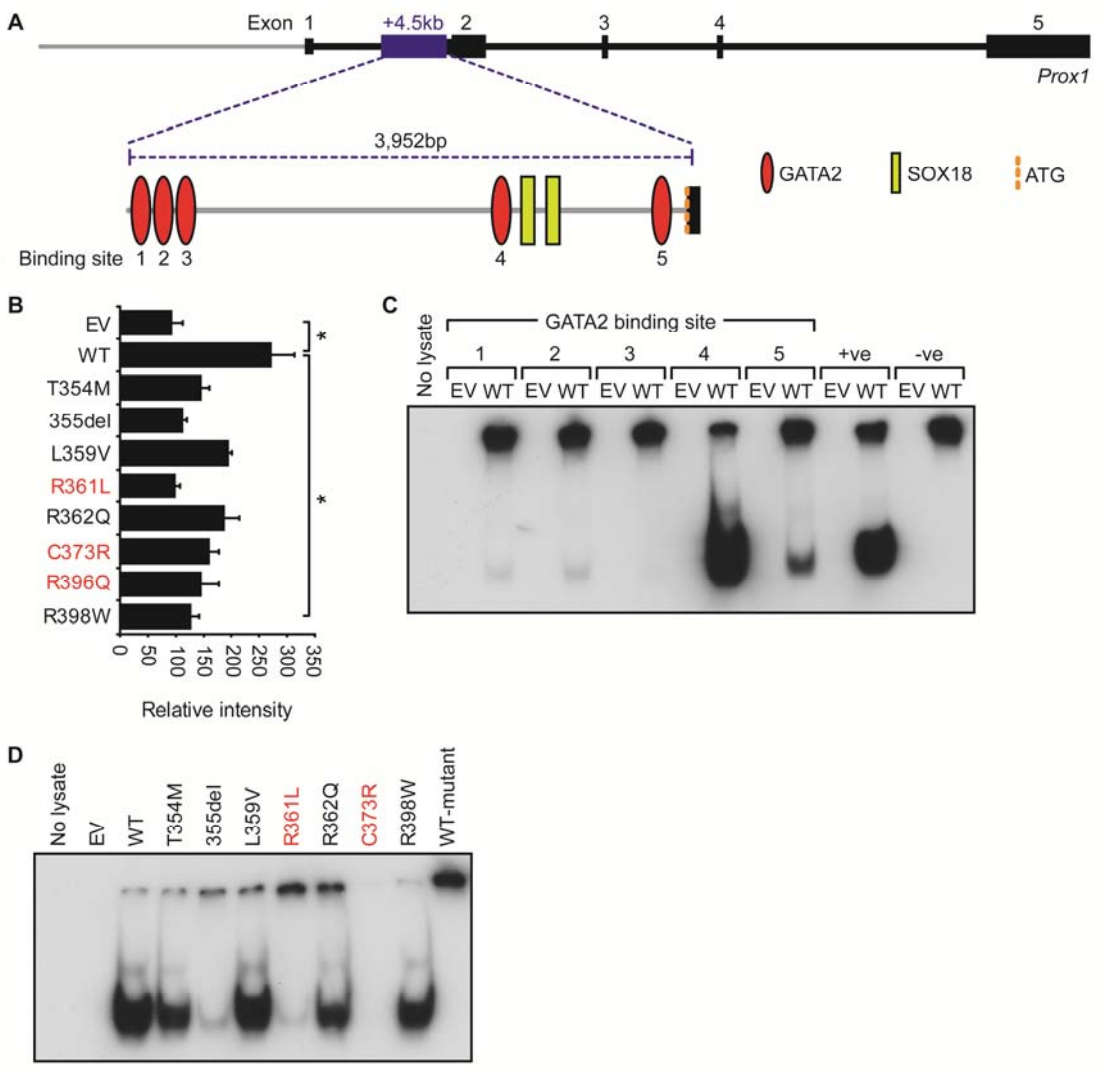

Supplemental Figure 1. GATA2 Emberger mutants have reduced capacity to bind and transactivate the *Prox1* +4.5 kb regulatory region.

(A) Schematic demonstrating location of *Prox1* +4.5 kb regulatory region relative to the *Prox1* gene and arrangement of 5 GATA and 2 SOX18 binding sites conserved between human and mouse. (B) HEK293 cells were transiently co-transfected with GATA2 (wild-type or mutant) expression constructs together with a *Prox1* +4.5 kb luciferase construct. Luciferase activity was measured after 24 hours. Error bars correspond to ± SEM, n = 3 independent experiments (one way ANOVA, *$p<0.05$ relative to WT GATA2). (C) WEMSA assay for GATA2 binding to each of the 5 consensus GATA sites in the *Prox1* +4.5 kb element indicate that site 4 bound GATA2 most strongly. (D) Binding of wild-type and mutant GATA2 proteins to the GATA site in *Prox1* +4.5 kb was assessed by WEMSA. *GATA2* mutations associated with lymphedema (red) demonstrate dramatically reduced capacity to bind (D) and transactivate (B) *Prox1* +4.5 kb. WT; wild-type, EV; empty vector control.

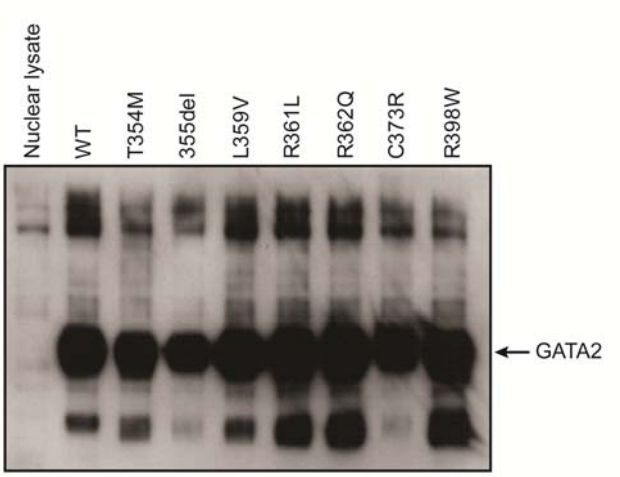

Supplemental Figure 2. WEMSA loading control. Immunoblotting of nuclear lysates was performed to ensure that comparable levels of wild-type and mutant GATA2 protein were present in all samples tested in the WEMSA assay.

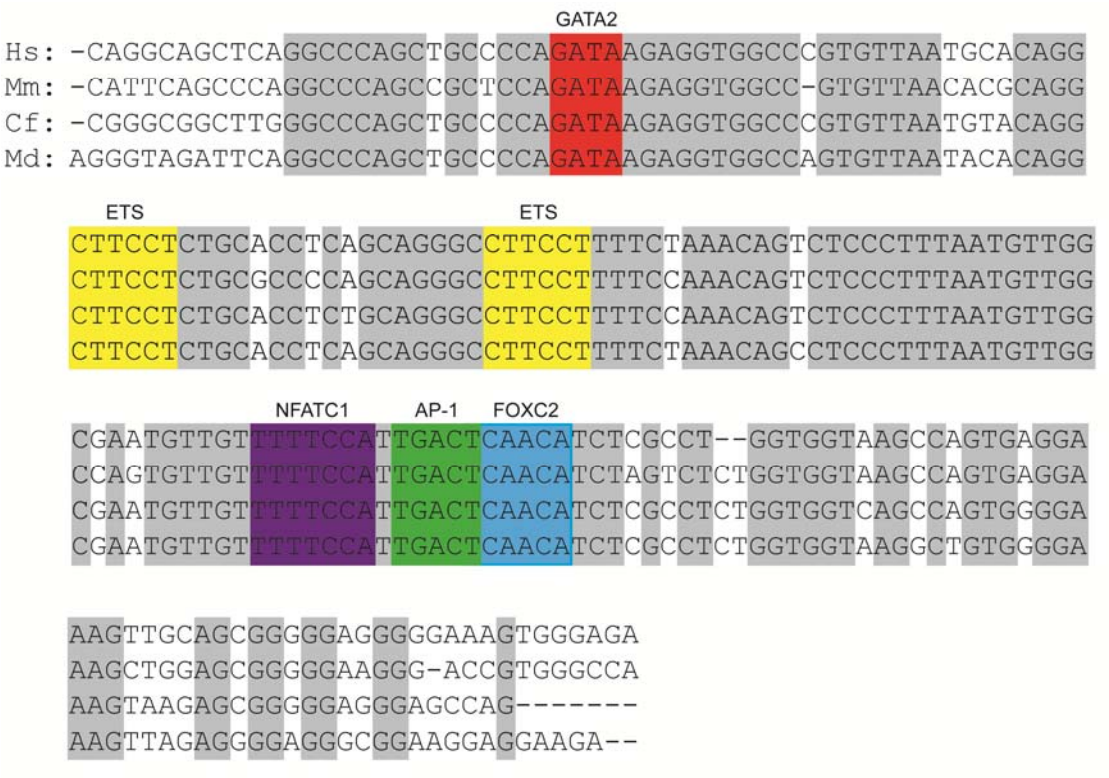

Supplemental Figure 3. Conserved consensus transcription factor binding sites in *PROX1* -11 kb. Aligned sequences across species, highlighting a region of high conservation (~150bp; grey shaded bases) in the *PROX1* -11 kb enhancer element that contains consensus binding sites for GATA2, ETS, NFATC1, AP-1 and FOXC2. Hs; *Homo sapiens*, Mm; *Mus musculus*, Cf; *Canis familiaris*, Md; *Monodelphis domestica*.

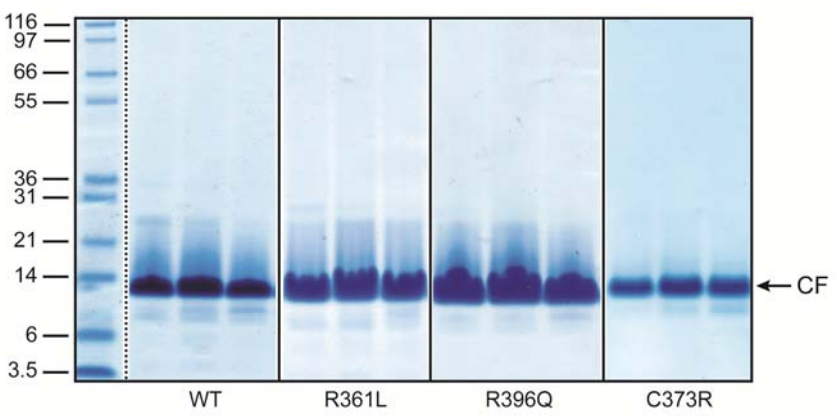

Supplemental Figure 4. SDS-PAGE analysis of purified GATA2 C-terminal zinc finger proteins. Samples of the retained fractions from the final (size-exclusion chromatography) stage of purification were run for WT and the three GATA2 Emberger mutant proteins, demonstrating that all proteins used for EMSA assays have similar levels of purity. Quantification of bands using ImageJ indicates >90% purity. Size standards (kDa) are shown on the left. The dashed line separates lanes taken from the same gel (intervening lanes removed for clarity), solid lines separate lanes taken from different gels. GATA2-CF; GATA2 C-terminal zinc finger.

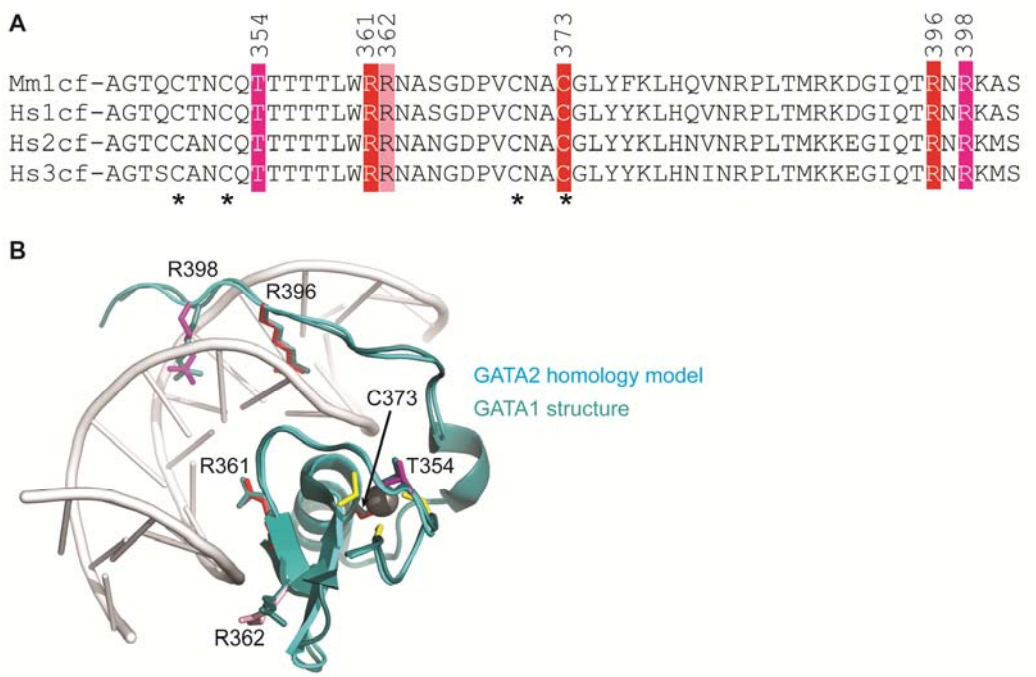

Supplemental Figure 5. Similarity of the C-terminal zinc fingers from GATA1-3. (A) Alignment of the GATA1-3 sequences from mouse (Mm) or Human (Hs) show high levels of sequence homology. All of the relevant mutated residues are fully conserved in this set of proteins with mutated residues highlighted based on their effect on GATA2-DNA binding: most affected (red), moderately affected (magenta), little or no effect (pink). Asterisks indicate zinc-coordinating residues. (B) Overlay of the GATA2 homology model (cyan) with the GATA1 structure (turquoise) in cartoon representation. Mutated side chains are shown in stick representation either in turquoise for GATA1 or coloured based on their effect on DNA binding: most affected (red), moderately affected (magenta), little or no effect (pink). The homology model of GATA2 bound to DNA was generated using Swiss-Model (http://swissmodel.expasy.org/) using the structure of GATA3 bound to DNA as a template (pdb accession code: 4HCA). This model (and the GATA3 template) is identical to the structure of GATA1 bound to the same core sequence (pdb accession code: 3VD6); the structures of all of the mutated residues are extremely highly conserved.

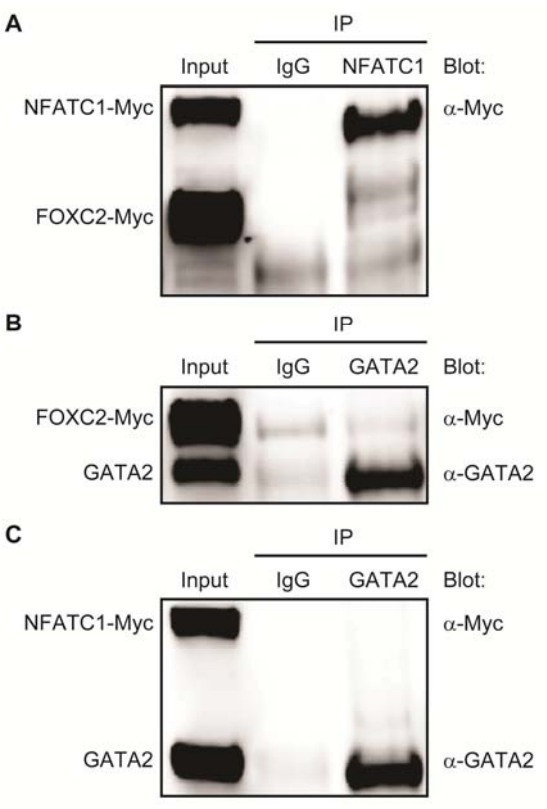

Supplemental Figure 6. Gata2 does not physically interact with Nfatc1 or Foxc2. HEK293 cells were co-transfected with (A) Nfatc1-Myc and Foxc2-Myc (B) Gata2 and Foxc2-Myc, or (C) Gata2 and Nfatc1-Myc expression constructs. Immunoprecipitation was performed with control IgG or indicated antibodies, followed by immunoblotting with anti-Myc and anti-GATA2 antibodies.

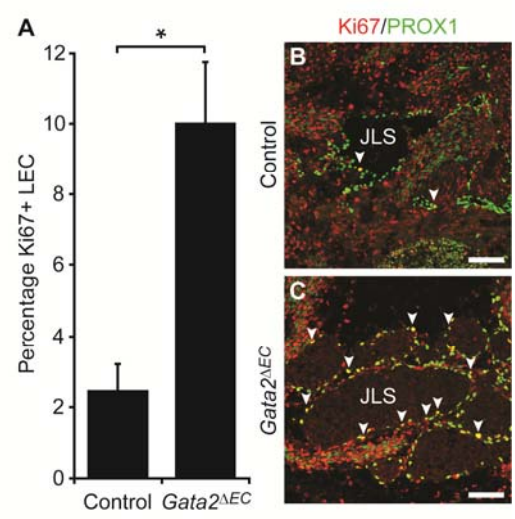

Supplemental Figure 7. Elevated LEC proliferation in the jugular lymph sacs of *Gata2*$^{\Delta EC}$ embryos.

(A) Immunostaining with Ki67 (a marker of proliferating cells) and Prox1 revealed an increase in the number of cells positive for both Prox1 and Ki67 (arrowheads) in the jugular lymph sacs (JLS) of E13.5 *Gata2*$^{\Delta EC}$ embryos compared to littermate controls (Cre negative;*Gata2*$^{flox/flox}$). Between 300 and 600 cells were counted per genotype. Error bars correspond to ± SEM (control embryos n = 3, *Gata2*$^{\Delta EC}$ embryos n = 5) across 3 litters (t-test, *$p<0.05$). (B) and (C) are representative images of the jugular lymph sacs of control and *Gata2*$^{\Delta EC}$ embryos, respectively. Note the multi-lobed, blood-filled lymph sacs in *Gata2*$^{\Delta EC}$ embryos (C). Scale bars represent 100μm.

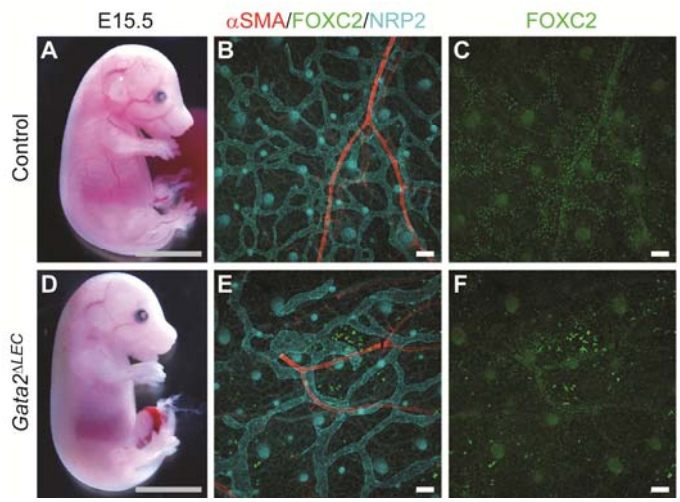

Supplemental Figure 8. Foxc2 levels are reduced in *Gata2*$^{\Delta LEC}$ embryos.
Prox1Cre^{ERT2}*;Gata2*$^{flox/+}$ male mice were crossed with *Gata2*$^{flox/flox}$ female mice and tamoxifen was administered at E13.5 and E14.5. Whole mount immunostaining of embryonic skin harvested at E15.5 (A, D) for alpha smooth muscle actin (αSMA; red), Foxc2 (green) and Nrp2 (cyan) revealed enlarged, irregular dermal lymphatic vessels (B, E) with a marked reduction in Foxc2 levels (C, F) in *Gata2*$^{\Delta LEC}$ embryos compared to control counterparts (Cre negative;*Gata2*$^{flox/flox}$). Grey scale bars represent 5mm. White scale bars represent 100μm.

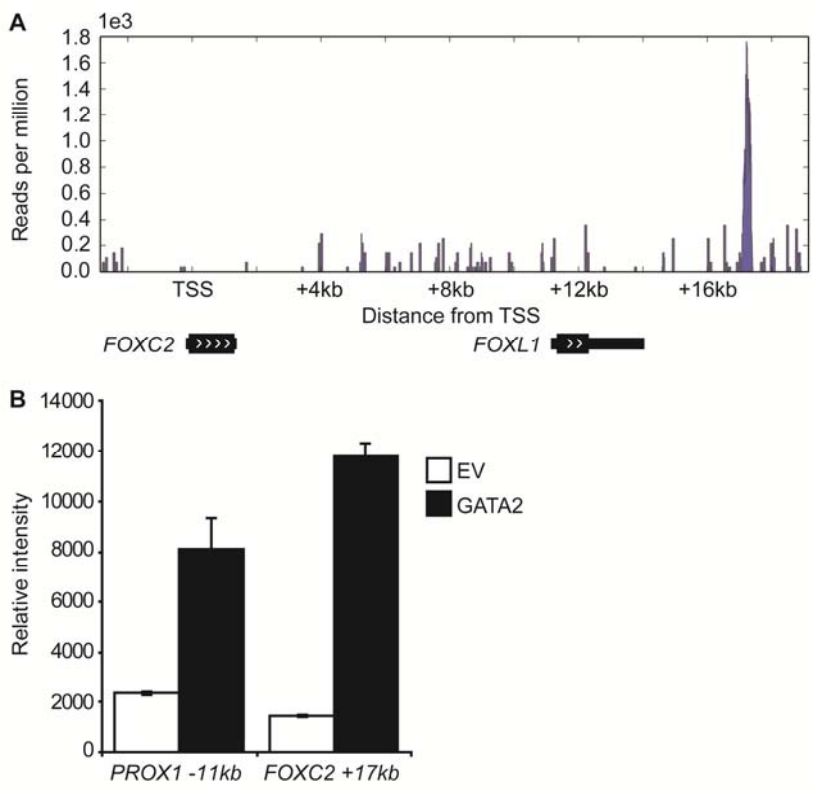

Supplemental Figure 9. GATA2 binds a potential regulatory element 17 kb downstream of *FOXC2*.

(A) ChIP-Seq profile demonstrating prominent GATA2 occupancy in the region of the *FOXC2* locus in hLEC. (B) HEK293 cells were transiently co-transfected with a wild-type GATA2 expression construct and a *FOXC2* +17kb luciferase reporter construct. Luciferase activity was measured after 24 hours. Error bars correspond to ± SD (n = 3) from one experiment.

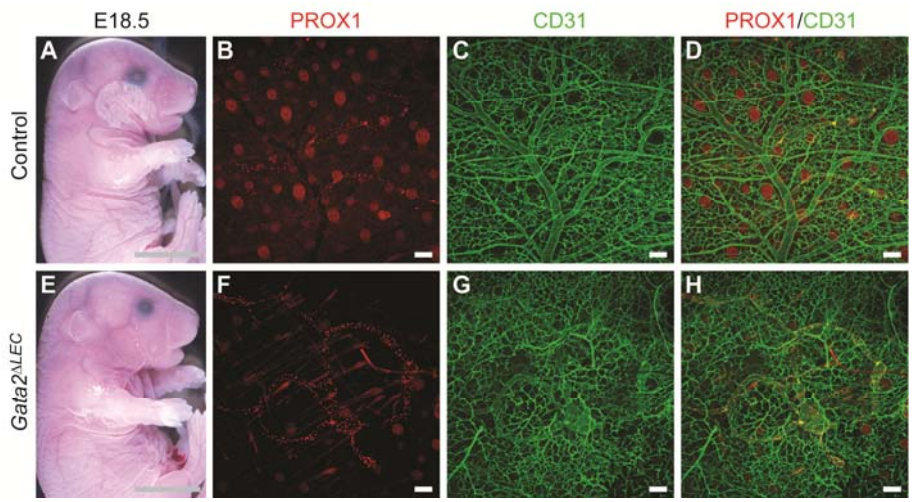

Supplemental Figure 10. Dermal lymphatic vessels in E18.5 *Gata2*$^{\Delta LEC}$ embryos are dilated and irregularly patterned.
Prox1Cre^{ERT2}*;Gata2*$^{flox/+}$ male mice were crossed with *Gata2*$^{flox/flox}$ female mice and tamoxifen was administered at E12.5, E13.5 and E14.5. Embryos harvested at E18.5 display no gross morphological phenotypes (A, E). Whole mount immunostaining of skin for Prox1 (B, F; red) and CD31 (C, G; green) revealed bulbous, irregularly patterned dermal lymphatic vessels in *Gata2*$^{\Delta LEC}$ embryos (F-H), compared to controls (Cre negative;*Gata2*$^{flox/flox}$, B-D). Grey scale bars represent 5mm. White scale bars represent 100μm.

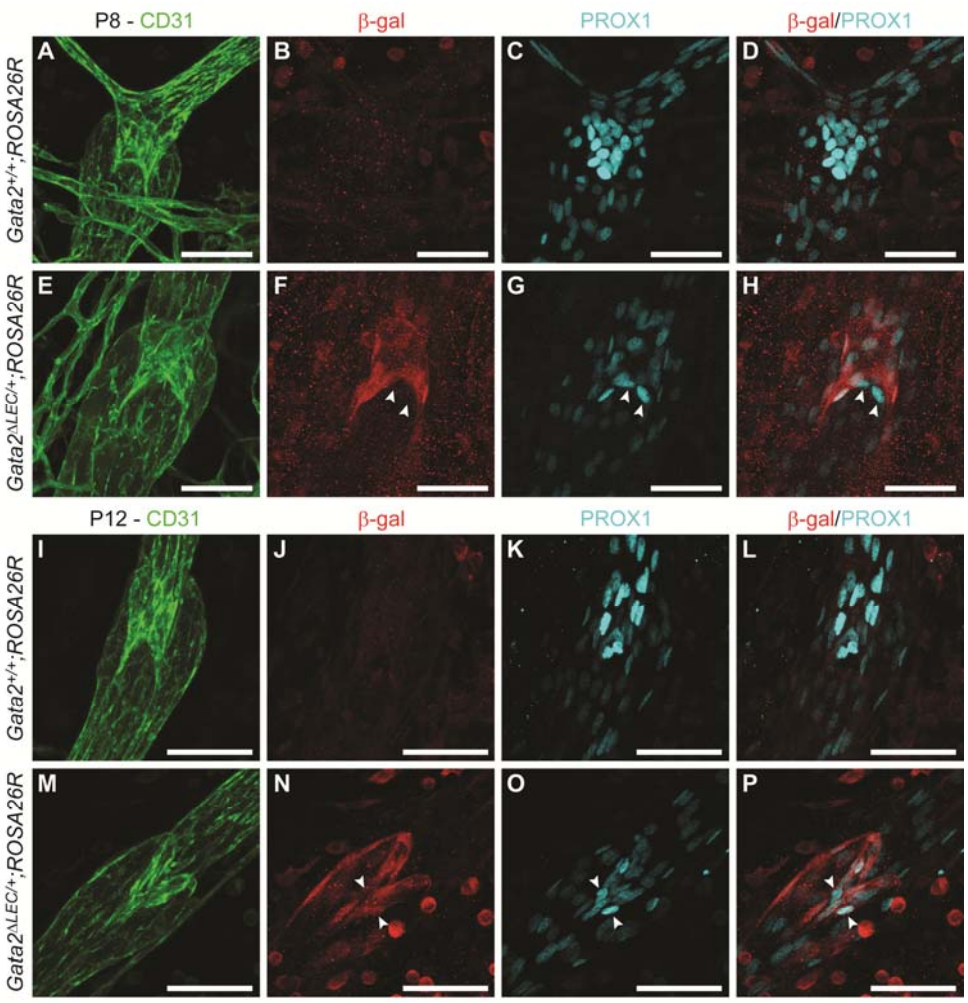

Supplemental Figure 11. Analysis of Cre activity in the lymphatic vessel valves of *Prox1Cre^{ERT2};Gata2$^{flox/+}$;ROSA26R* mice.
Prox1Cre^{ERT2};Gata2$^{flox/+}$;ROSA26R and littermate control (Cre negative;*Gata2$^{flox/+}$;ROSA26R*) pups were injected with tamoxifen at P4. Whole mount immunostaining of mesenteries at P8 (A-H) and P12 (I-P) with antibodies to β-galactosidase (red), Prox1 (cyan) and CD31 (green) demonstrated efficient Cre activity in lymphatic vessel valves. Prox1 levels were reduced in the valves of *Prox1Cre^{ERT2};Gata2$^{flox/+}$;ROSA26R* mice (G, O). Low β-galactosidase levels correlated with cells retaining high Prox1 levels (F-H, N-P, arrowheads). Scale bars represent 50μm.